Three organic/inorganic nanolayers on flexible foam allow retaining superior flame retardancy performance upon mechanical compression cycles

frontiers in Materials

ORIGINAL RESEARCH
published: 27 February 2019
doi: 10.3389/fmats.2019.00020

Three Organic/Inorganic Nanolayers on Flexible Foam Allow Retaining Superior Flame Retardancy Performance Upon Mechanical Compression Cycles

Federico Carosio and Alberto Fina*

Dipartimento di Scienza Applicata e Tecnologia, Politecnico di Torino, Alessandria Campus, Alessandria, Italy

The water-based deposition of flame retardant coatings on flexible polyurethane foams has attracted great interest among the scientific community due to the great performances associated with this technology. Unfortunately, this approach results inefficient as it requires a high number of steps in order to achieve the desired properties. In this paper, we report the production of flame-retardant foams by means of the simple deposition of only three nanoparticles containing layers. The composition and order of the deposited layer has been designed in order to provide specific flame retardant actions, targeting the delayed release of polymer decomposition products to the gas phase, the dilution of these flammable products with water, and the intumescent barrier formation. The morphology of the coated foams after the adsorption of each layer has been investigated by scanning electron microscopy, demonstrating the ability of each adsorbed layer to completely wrap the complex 3D structure of the foam. This three layers-based coating produces a protective exoskeleton that is capable of self-extinguishing the flame in standard flammability tests, leaving the foam almost unaffected (final residue 98%). In forced combustion tests by cone calorimetry, treated foams showed considerably reduced combustion rates, with reduced peak of heat release rate (−50%) as well as consistent reduction in the smoke optical density (−51%) and the total smoke release (−34%). In addition, treated foams have been demonstrated to maintain the ability to self-extinguish the flame as well as reduced combustion rates and smoke production even after being subjected to 100 compression cycles.

Keywords: layer-by-layer, flexible polyurethane foams, boehmite, montmorillonite, ammonium polyphosphate, flame retardancy

OPEN ACCESS

Edited by:
Alessandro Pegoretti, University of Trento, Italy

Reviewed by:
José-Marie Lopez-Cuesta, Institut Mines -Télécom Mines Alès, France
Mustapha Kaci, University of Béjaïa, Algeria

****Correspondence:***
Federico Carosio
federico.carosio@polito.it

Specialty section:
This article was submitted to Polymeric and Composite Materials, a section of the journal Frontiers in Materials

Received: *30 November 2018*
Accepted: *04 February 2019*
Published: *27 February 2019*

Citation:
Carosio F and Fina A (2019) Three Organic/Inorganic Nanolayers on Flexible Foam Allow Retaining Superior Flame Retardancy Performance Upon Mechanical Compression Cycles. Front. Mater. 6:20. doi: 10.3389/fmats.2019.00020

INTRODUCTION

Recent trends in materials science have clearly pointed toward the production of green and environmentally friendly material concepts capable of improving sustainability while also delivering optimized and competitive performances. To this aim, research has been focused on the exploitation of natural resources (e.g., nanocellulose, natural fibers etc.) and water-based processes in different application fields (Mohanty et al., 2002; Klemm et al., 2011). The fire safety of polymeric materials represents an area of concern; indeed, due to their organic nature, polymers can easily ignite after accidental exposure to small flames or irradiation at high heat

fluxes, leading to catastrophic fire events. Current concerns about the toxicity of some commonly used flame retardant (FR) chemicals (halogen-based) (Stapleton et al., 2011), coupled with recent tragic events involving flammability of non-flame retarded polymer foams (Rawlinson et al., 2017), have been presented to broad audiences of non-experts. This clearly increased societal awareness on the problem of halogen-based FR and the need for safer and better performing alternatives. A possible solution is represented by the exploitation of a nanotechnological approach in which the surface of flammable items (i.e., fabrics and open cell polyurethane foams, PU), is modified with nanostructured coatings deposited by means of green water-based deposition processes (Malucelli et al., 2014; Alongi et al., 2016). Among the possible different approaches, the Layer-by-Layer (LbL) deposition technique represents one of the most widely employed surface modification tool to achieve flame retardancy properties (Holder et al., 2017). Nanostructured coatings are LbL-assembled on the surface following the alternate adsorption of oppositely charged species from aqueous based solutions/suspensions (Decher and Schlenoff, 2012). One of the key advantages of LbL is certainly its versatility in both the components selection and deposition parameters. Indeed, for virtually any combination of water-soluble polyelectrolytes and water-stable nanoparticles, it is possible to find suitable deposition conditions (e.g., time, temperature, concentration, pH) that allow for a steady coating buildup (Hammond, 2004). Thanks to its versatility, the LbL deposition has been applied to various substrates, including textiles, foams and thin films, and the effects of pH, ionic strength and molecular weight on the achieved FR properties have also been investigated (Laufer et al., 2012; Carosio et al., 2015c, 2018a). Although the concept of LbL-assembled FR coatings was first validated on fabrics, open cell foams have recently attracted great interest as a substrate to protect due to their inherently high flammability, which makes them one of the first items to be ignited during a fire (Ahrens, 2008). Different coating compositions and FR strategies have been investigated, mainly targeting the deposition of nanoparticles-rich coatings characterized by brick and mortar structures or the assembly of organic polyelectrolytes with intumescence-like behavior (Carosio et al., 2014b, 2018c; Smith et al., 2017). These two FR concepts have also been combined together using nanoparticles as reinforcing agents either within the intumescent coating or below it in stacked configurations (Cain et al., 2013; Holder et al., 2015). Treated foams usually achieve considerably reduced combustion rates and, in some cases, the ability to stop flame spread during flammability tests. Self-extinguishing typically requires a high number of deposition steps (usually >10), which is currently preventing the scale-up and large scale industrial exploitation of the LbL approach (Richardson et al., 2015; Carosio and Alongi, 2016). In addition, the durability of the LbL coating during repeated foam deformation has never been properly addressed. This represents another strong limitation of the state of the art, as one of the main applications of soft open cell PU foams is in upholstered furniture for buildings and transportations. In the present paper, we aim at the design of a coating composition and its assembly onto a soft PU foam in order to obtain highly performing and durable FR coatings, with only three depositions steps. To this aim, open cell PU foams have been treated, following the procedure schematized in **Figure 1**.

Each deposition step deposits a nanoparticle/polyelectrolyte layer with specific FR characteristics. The hypothesis is that the first layer made of polyacrylic acid and montmorillonite may produce a "brick and mortar" structure to reduce volatile feed to the gas phase, while providing stability to the remaining portion of the coating (Carosio et al., 2015a). In the second layer, boehmite (BOH) nanoparticles deposited within a poly(diallyldimethylammonium chloride) (PDAC) may release water during combustion (with volatile dilution and cooling effects) while also leaving an inorganic protective layer made of aluminum oxide (Rothon and Hornsby, 2014). The outermost layer made of ammonium polyphosphate (APP) and montmorillonite (MMT) acts as inorganic intumescent layer producing an expanded silicoalluminophosphate barrier (Alongi and Carosio, 2016). The resulting coating morphology has been evaluated by scanning electron microscopy while the resulting FR properties have been assessed by horizontal flammability and cone calorimetry tests. Furthermore, in an effort to evaluate the coating durability, treated foams have been subjected to deformation cycles evaluating the effects on coating morphology and FR properties.

MATERIALS AND METHODS

Materials

Open cell polyurethane foams (PU) with a density of 18 g/dm^3 and thickness of 18 mm were purchased from a local warehouse. The as received foams were washed by dipping and vigorous squeezing in deionized water in order to remove dust and processing residues and then dried in a ventilated oven at the temperature of 70°C. Poly(diallyldimethylammonium choride) (PDAC, average Mw 400,000–500,000, 20% wt in H_2O), polyacrylic acid (PAA, solution average Mw ∼100,000, 35% wt. in H_2O), Sigma-Aldrich. The sodium montmorillonite (MMT) was purchased from Southern Clays. Ammonium polyphosphate (PHOS-CHEK® P30) was purchased from ICL Performance Products, Inc. Bohemite nanoparticles (Dispal 10F4) with average dispersed size 240 nm (as declared by the producer) have been supplied by Sasol. Ultrapure water (18.2 MΩ) supplied by a Q20 Millipore system was employed for the preparation of the solutions and suspensions employed in this work. Both PAA/MMT and PDAC/BOH have been employed to prepare a 3% wt suspension with 1:2 polyelectrolyte/nanoparticle ratio. The suspension was prepared by firstly diluting the polyelectrolyte solution and then adding the required amount of nanoparticles. APP and MMT have been employed with a 2:1 polyelectrolyte/nanoparticle ratio for the preparation of a 3% wt water suspension.

Layer-by-Layer Deposition

The prewashed PU foam has been treated with a three-step deposition process as schematized in **Figure 1**. First the foam was dipped in the PAA/MMT bath (negative suspension), then

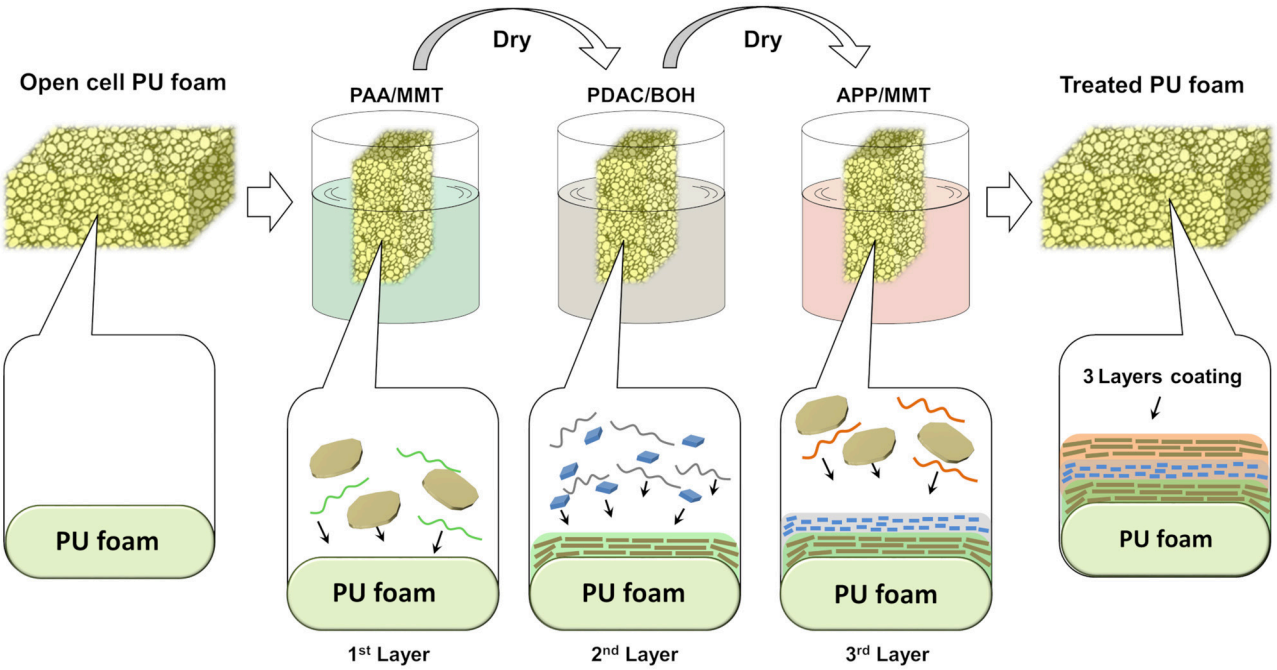

FIGURE 1 | Schematization of the coating procedure employed in this study. PU foams are dipped in three different baths following the order: polyacrylic acid/montmorillonite (PAA/MMT) suspension, poly(diallyldimethylammonium chloride)/boehmite (PDAC/BOH), and ammonium polyphosphate/montmorillonite (APP/MMT). This process deposits a three-layer coating.

in the PDAC/BOH bath (positive suspension) and eventually in the APP/MMT bath (negative suspension). During each deposition step, the foam is dipped in the bath and vigorously squeezed in order to fill its internal structure with the suspension. After an immersion time of 10 min, the wet foam was removed from the bath, squeezed to remove the excess of suspension and dried in a ventilated oven at 70°C. The process as shown in **Figure 1** deposits a three layer coating (PAA/MMT)/(PDAC/BOH)/(APP/MMT) on the PU structure. The mass gain, evaluated by weighting the samples before and after the LbL deposition, was 37 ± 3%. In the following, a sample coated with three layers is denoted as PU-3 L.

Characterization

The morphology of untreated and treated PU foams was investigated using a LEO^{-1}450VP Scanning Electron Microscope (SEM) operating at 5 kV. Small pieces (∼10 × 10 × 5 mm^3) of PU foams were positioned on conductive adhesive tape and gold coated prior to observation. Fourier Transformed-Infrared spectra in attenuated total reflectance (FT-IR ATR) were collected at room temperature in the range of 4,000–700 cm^{-1} (16 scans and 4 cm^{-1} resolution) using a Perkin Elmer Frontier spectrometer equipped with a diamond crystal. In order to preliminarily evaluate the coating durability during foam deformation, simple compression cycles have been performed on coated PU samples as schematized in **Supplementary Figure 1**. During the test the foam is placed between two 1 mm thick aluminum plates and then manually compressed by the action of a weight placed on top of the plate resulting in 16 kPa pressure[1]. The compression is maintained for 5 s after which the weight is removed in order to let the foam recover its original shape. Then, after 10 s the weight is applied again in order to perform a second compression cycle. This cycle has been repeated 50 and 100 times. In the followings, samples coded as PU-3 L @50 c and PU-3 L @100 c refer to a coated foam subjected to 50 and 100 compression cycles, respectively.

Flammability tests were performed in horizontal configuration. 50 × 150 × 15 mm^3 specimens positioned on a metallic grid were ignited by applying a 20 mm blue methane flame on the short side of the sample. The flame was applied for 6 s. During the test, the formation of incandescent droplets of molten polymer (melt dripping) was evaluated by placing dry cotton underneath the sample. The time, in seconds, a flame persisted on the sample after the igniting source has been removed was recorded as flaming time. The percentage of mass left at the end of the test is reported as final residue and was evaluated by weighting the sample before and after the test. Three different samples were tested for each formulation. Forced combustion tests were performed by cone calorimetry (Fire Testing Technology). 50 × 50 ×18 mm^3 specimens were exposed to a 35 k W/m^2 radiative heat flux. Average values concerning Time To

[1](i.e., ∼163 g/cm^2, roughly simulating the weight of a person, despite a full mechanical deformation study would require a more complex setup, well beyond the scope of this study).

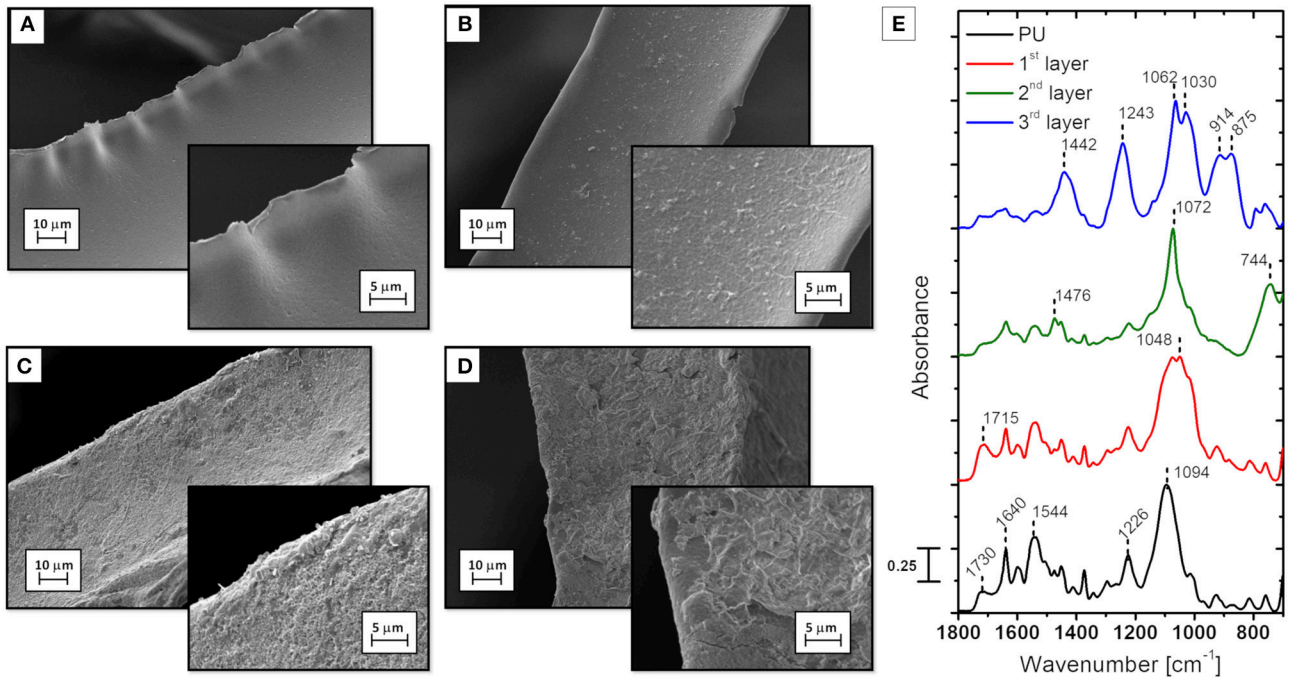

FIGURE 2 | SEM micrograph of untreated and treated PU foam (main: 1000X, inlet: 2500X): **(A)** neat PU, **(B)** 1st layer, **(C)** 2nd layer, **(D)** 3rd layer, and **(E)** ATR spectra of neat PU and PU coated with 1, 2, and 3 layers.

Ignition (TTI), peak of Heat Release Rate (pkHRR), Total Heat Release (THR), average Specific Extintion Area (SEA), Total smoke release (TSR) and final residue were evaluated and are presented with their experimental deviations. Measurements were performed four times for each formulation. Prior to flammability and forced combustion tests, all specimens were conditioned in a climatic chamber (23 ± 1°C 50% R.H) for 48 h.

RESULTS AND DISCUSSION

Coating Morphology

The changes in surface morphology and chemical composition of small samples of PU foam after each deposition step have been investigated by SEM and ATR spectroscopy. **Figure 2** reports collected micrographs and IR spectra. In **Figure 2** a sample coded as PU 1st layer denotes the deposition of only the (PAA/MMT) layer, PU 2nd layer denotes the deposition of the (PAA/MMT)/(PDAC/BOH) layers and PU 3rd layer denotes the deposition of the (PAA/MMT)/(PDAC/BOH)/(APP/MMT) layers (i.e. the complete coating structure).

The unmodified PU shows a typical open cell structure where cell walls generated during the foaming process are characterized by a smooth and even morphology (**Figure 2A**). The deposition of the PAA/MMT layer (8 ± 1% add-on) completely changes the foam walls morphology. Indeed, the formation of a thin and homogeneous coating containing MMT nanoplatelets embedded within a PAA matrix can be easily observed in **Figure 2B**. This is in agreement with previously reported LbL assemblies comprising polyelectrolytes and MMT (Carosio et al., 2014a). The deposition of the second PDAC/BOH layer (20 ± 3% total add-on) provides an additional change, and BOH nanoparticles are evenly distributed on every surface available producing a granular morphology as reported in high magnification micrographs in **Figure 2C**. The final deposition step adds the APP/MMT layer (37 ± 3% total add-on) and this corresponds to another change in surface morphology that appears to have higher rugosity (**Figure 2D**). It is worth observing that, starting from the first deposition step, the PAA/MMT coating completely covers all the surfaces available without displaying an island growth that is typical of LbL assemblies at early deposition steps. This can be ascribed to the good affinity between the PAA and the PU surface, where extensive hydrogen bonding between the urethane bonds and undissociated carboxylic acids of PAA may occur (Laufer et al., 2013). The stability and homogeneity of this first adsorbed layer is fundamental for the proper depositions of the subsequent layers. The resulting coating creates a complete protective exoskeleton that completely wraps the 3D structure of the foam without altering its open cell nature as reported in low magnification micrographs collected in **Supplementary Figure 2**. ATR spectroscopy has been also employed to evaluate the change in surface chemistry after each adsorption step (**Figure 2E**). Neat PU shows characteristic signals associated to C=O vibrations related to the urethane (broad peak centered at 1,730 cm^{-1}), urea group (1,640 cm^{-1}), N–H and C–N vibrations of the urethane and urea groups (band centered at 1,544 cm^{-1}) and C–O–C asymmetric and

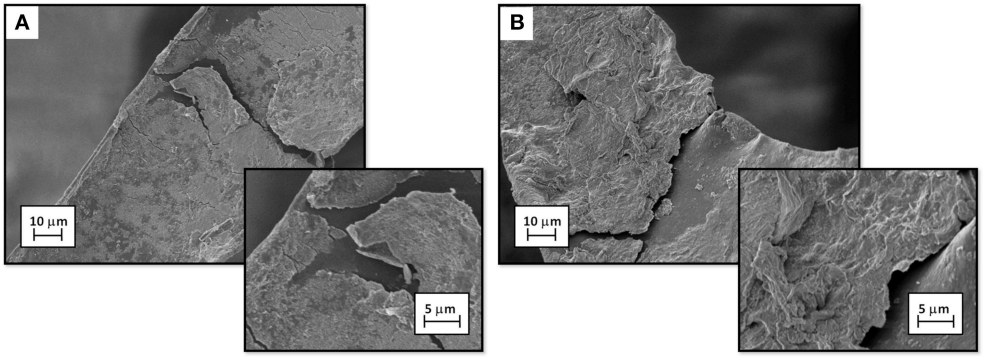

FIGURE 3 | SEM micrographs (main: 1000X, inlet: 2500X) of PU-3 L foam after 50 **(A)** and 100 **(B)** compression cycles.

symmetric vibrations (1,226 and 1,094 cm^{-1}, respectively) (Gómez-Fernández et al., 2016). The neat coating constituents have been also analyzed, and collected spectra are reported in **Supplementary Figure 3**. Pure PAA shows characteristic C=O and C-O-C signals at 1,700 and 1,164 cm^{-1}, respectively (Dong et al., 1997). MMT displays the strongest peak centered at 1,000 cm^{-1} and ascribed to Si-O vibrations (Madejová, 2003). PDAC shows the main characteristic bands associated to C-H bonds in CH_2 (1,470 cm^{-1}) and N-C bonds (1,122 cm^{-1}) (Sun et al., 2008). BOH asymmetric and symmetric Al-OH vibrations are found at 1,153 and 1,075 cm^{-1}, respectively (Haghnazari et al., 2014). This latter peak also accounts for Al-O vibrations while OH groups are evidenced by the peak at 738 cm^{-1} (Guido et al., 2013). APP shows characteristic peaks associated to P=O (1,245 cm^{-1}), P-O (1,062 and 1,022 cm^{-1}), P-O^- (880 cm^{-1}), and N-H of ammonium ions (1,423 cm^{-1}) (Socrates, 2006). When the first PAA/MMT layer is deposited on PU foams, the characteristic peaks of the substrate change consistently, evidencing the formation of new peaks at 1,715 and 1,048 cm^{-1} ascribed to C=O stretching in PAA and Si-O-Si vibrations in MMT, respectively. The deposition of the second layer results in the appearance of signals associated to CH_2 vibration (1,476 cm^{-1}) in PDAC as well as Al-O/Al-OH (1,072 cm^{-1}) and O-H vibration (744 cm^{-1}) in BOH. The presence of the last layer is evidenced by signals mainly associated to APP such as P=O (1,243 cm^{-1}), P-O (1,062 cm^{-1}), P-O^- (914 and 875 cm^{-1}) and N-H (1442 cm^{-1}), while MMT contributes with the signal at 1,030 cm^{-1}. It is worth mentioning that in the assembled layers many signals associated to polar functional groups of adsorbed species are shifted to different wavenumbers with respect to the neat products. The most apparent is the P-O- signal of APP that appears with two distinct peaks at 914 and 875 cm^{-1}, likely ascribed to P-O- interactions with PDAC and ammonium ions, respectively. The Si-O signal of MMT appears at higher wavenumbers as a consequence of hydrogen bond interactions with the co-adsorbed polyelectrolytes (i.e., PAA and APP; Chen and Zhang, 2006). In order to evaluate the durability of the coating, the foams treated with three layers have been subjected to repeated compression tests as described in the Materials and Methods section.

The morphology of the coating after 50 and 100 compression cycles has been evaluated by SEM, see **Figure 3** for collected micrographs. The deformation cycles impart strong deformations to the deposited coating that must comply to the change in shape of the substrate. Due to the ionic bonds in between the adsorbed layers and the nanoparticle-based structure, the deposited coating is inevitably rigid and the cyclic deformation results in the formation of cracks where portion of the assembly are partially detached from the substrate (**Figures 3A,B**). Interestingly, no visible differences in terms of damage extent can be appreciated when comparing the coating morphologies after 50 and 100 deformation cycles. This suggests that the cracks that are clearly visible in **Figures 3A,B** are generated during the first compression cycles in order to allow the foam walls to completely collapse upon compression. SEM investigations performed on PU-3 L samples after the first compression cycle support this as reported in **Supplementary Figure 4** where low magnification micrographs clearly show extensive cracks formation with minimal detachment of the coating. This is also confirmed by practical observations of the coated foams that are firmer after the deposition of the coating, but after few deformation cycles no significant qualitative differences can be observed when compared to the untreated foam. Such behavior is in agreement with previously reported literature (Li et al., 2013) where LbL-treated foams partially recovered the original stress/strain curve after few compression cycles. This is particularly important for the application in upholstered furniture and seats, allowing to preserve the comfort feeling for which the pristine foam was designed.

Flammability

Since PU foams represent one of the first items to be ignited during the start of a fire, it is mandatory to evaluate the flammability properties by means of horizontal flame spread tests. This test simulates the accidental exposure of the foam to a small flame thus allowing for the evaluation of the potential fire starting capability associated with the sample. **Figure 4** summarizes collected flammability parameters as well as snapshots of neat and coated foams during the test. Numerical

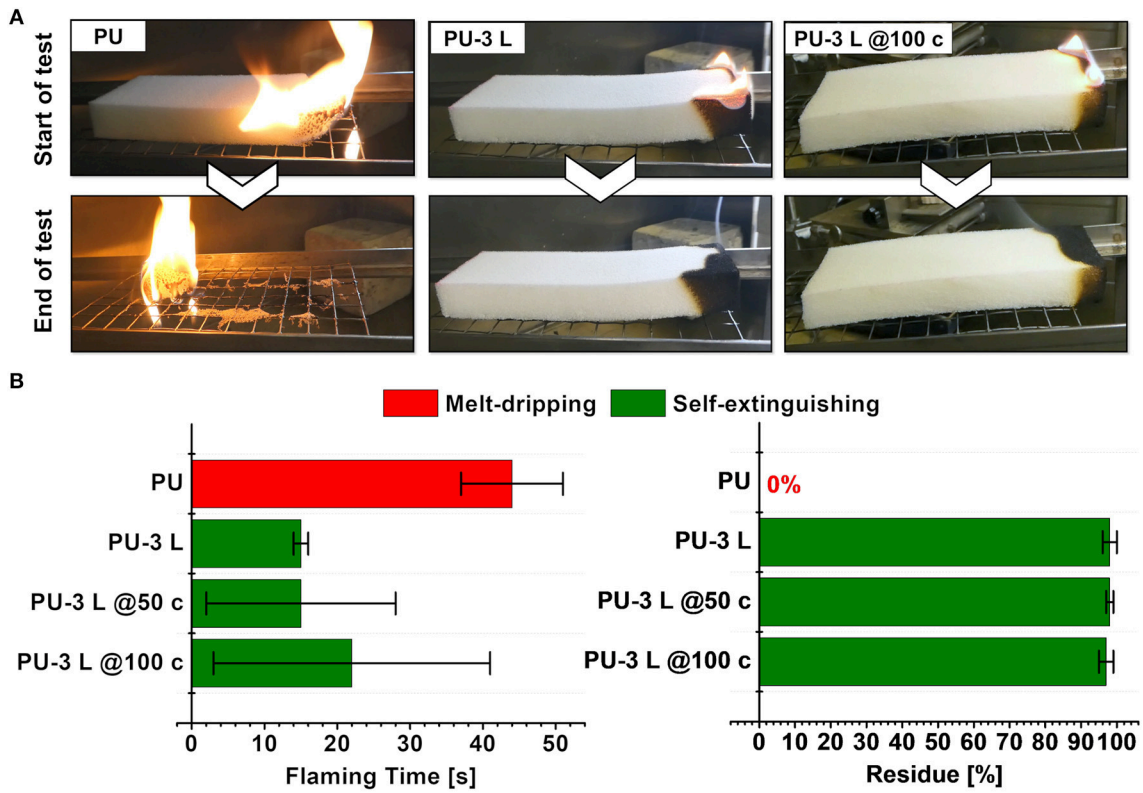

FIGURE 4 | Flammability tests performed on neat PU, treated PU, and treated PU foams after compression cycles; **(A)** snapshot of samples during the test, **(B)** flaming time and final residue.

parameters with their standard deviation are reported in **Supplementary Table 1**.

The uncoated PU foam can be easily ignited by the methane flame. When the ignition source is removed, the flames grow in size and rapidly spread to the entire length of the sample, completely consuming it (**Figure 4A**). During combustion, a vigorous melt dripping ignites the dry cotton placed underneath the sample. This phenomenon is typical of flexible PU foam and is related to the formation of flaming droplets of molten polymer that pose additional fire risks as not only the foam can be quickly ignited, but also the melt dripping can easily spread the fire to other ignitable materials. The presence of the three-layer coating completely changes this burning behavior. Indeed, upon removal of the ignition source, only a small flame remains confined in the first 2 cm of the foam, constantly reducing in size until it extinguishes within few seconds. No melt dripping is observed, and the residue collected at the end of the test accounts for 98% of the original mass. A nearly identical behavior is observed in coated foams subjected to 50 and 100 deformation cycles. Only a slight increase in the average flaming time was observed for compressed foams, meaning that self-extinguishing takes slightly longer to occur, but the deviation of burning times obtained for different specimens is considerably increased, suggesting a dependency on local density of defects. Nevertheless, all coated foams are capable of stopping flame spread and suppress the melt dripping phenomenon, yielding final residues within 97–98%. These results clearly point out the improved fire safety achieved by the deposited coatings. Indeed, thanks to the engineered structure of the three layers, the protective exoskeleton is able to prevent foam melting and collapsing while at the same time considerably reducing the release of volatile gasses that feed and sustain the flame. The resulting FR action is very efficient as self-extinguishing behavior is achieved with only three deposition steps. In addition, it seems that the formation of cracks during deformation cycles had rather limited effects on the FR performances of the coated foam.

Cone Calorimetry

Cone calorimetry tests allow to evaluate the reaction of untreated and treated foams when exposed to heat fluxes typically obtained in developing fires, thus assessing the contribution of the samples to fire growth and spread. During the test, samples are exposed to 35 kW/m^2 (i.e., heat flux related to early stages of a developing fire; Schartel and Hull, 2007), which triggers thermal degradation processes and the subsequent release of flammable volatiles that, when the proper concentration is reached, can be ignited by a spark igniter leading to flaming combustion. The instrument measures parameters associated to heat and smoke release. **Figure 5** collects HRR plots and histograms of the main parameters evaluated during the test

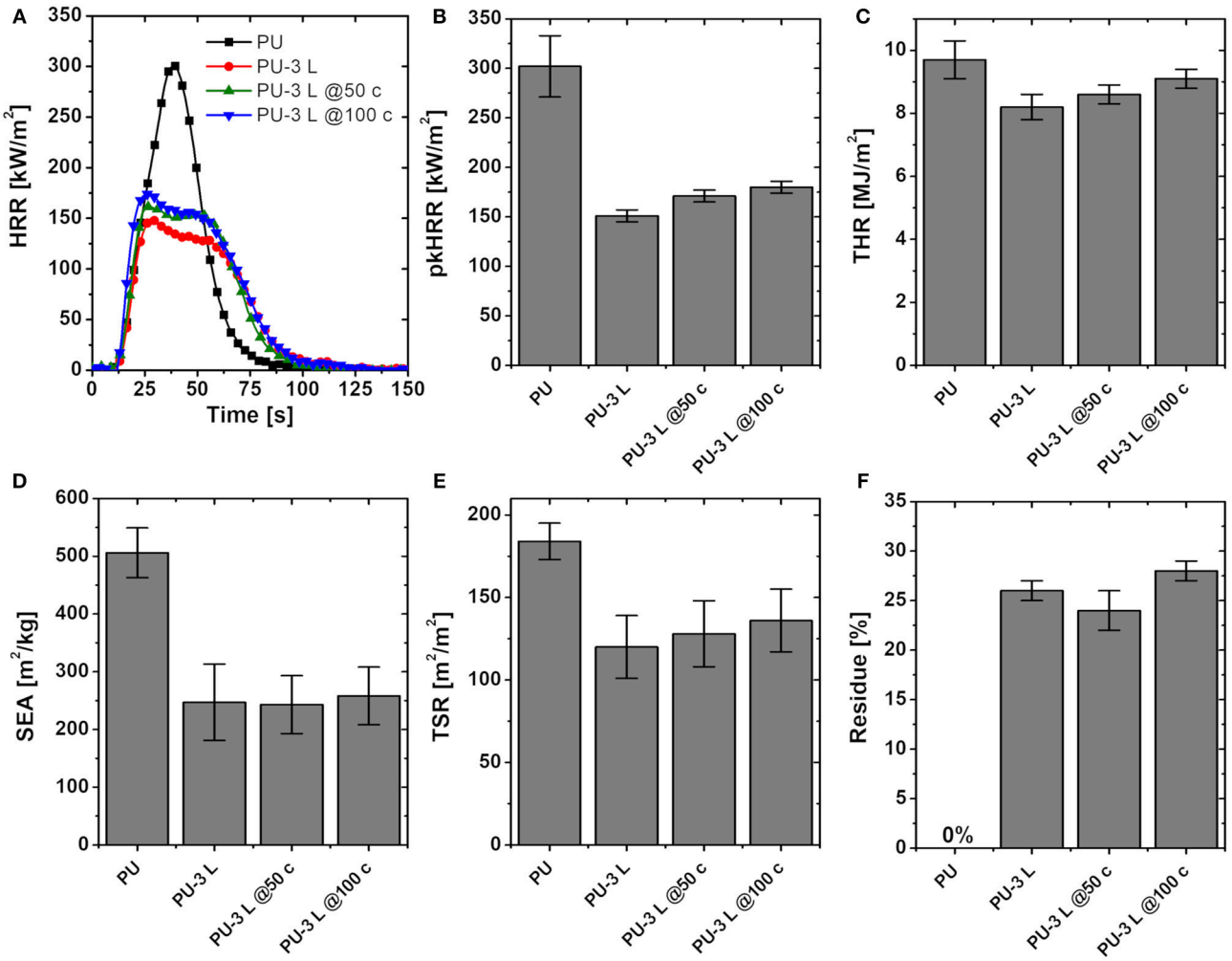

FIGURE 5 | Cone calorimetry parameters neat PU, treated PU, and treated PU foams after compression cycles: **(A)** HRR vs. time plot, **(B)** peak of heat release rate (pkHRR), **(C)** total heat release (THR), **(D)** average specific extinction area (SEA), **(E)** total smoke release (TSR), and **(F)** final residue.

while numerical values with their standard deviation are reported in **Supplementary Table 2**.

Upon exposure to the cone calorimetry heat flux, the neat PU foams show a quick ignition (TTI=2 s) followed by the foam structural collapse and the formation of a molten pool of a low viscosity liquid. This latter step produces a steeply increase in heat release rate that reaches the maximum value of about 300 kW/m^2 (**Figure 5A**, HRR vs. time plots). The behavior of flexible PU foam during cone testing is well documented and the collapsing and melting stages are normally associated to increased fire spreading risks (Kramer et al., 2010). The presence of the three-layers coating completely changes the burning behavior of coated PU foams. Indeed, upon ignition no structural collapse is observed and the foams maintain their original shape at the end of the test (see **Supplementary Figure 5**). Heat release rates are considerably reduced as demonstrated by a −50% in pkHRR value (**Figure 5B**, pkHRR histograms); on the other hand, the effect on THR values is rather limited, suggesting combustion of the PU is complete, yet delayed in time. Interestingly, a positive effect on smoke related parameters is also observed. Indeed, smoke optical density (SEA) and total smoke produced (TSR) are considerably reduced: −50 and −34%, respectively (**Figures 5D,E**). The final residue is increased to 25% of the starting mass. These results point out that the presence of the coating not only can efficiently reduce the rate of combustion and potential fire spread risk, but can also influence the production of smoke. Such observation is of crucial importance since it is reported that people are normally confronted with smoke and its effects during evacuation (Frantzich, 1994). The presence of dense smoke considerably increases escaping times while also causing loss of ability to react, unconsciousness, slower walking speed and long-term damage such as lung cancer (Gann, 2004). For these reasons, smoke-related effects represent an important cause of fire fatalities. Furthermore, coated foams subjected to 50 and 100 deformation cycles maintain performances similar to the

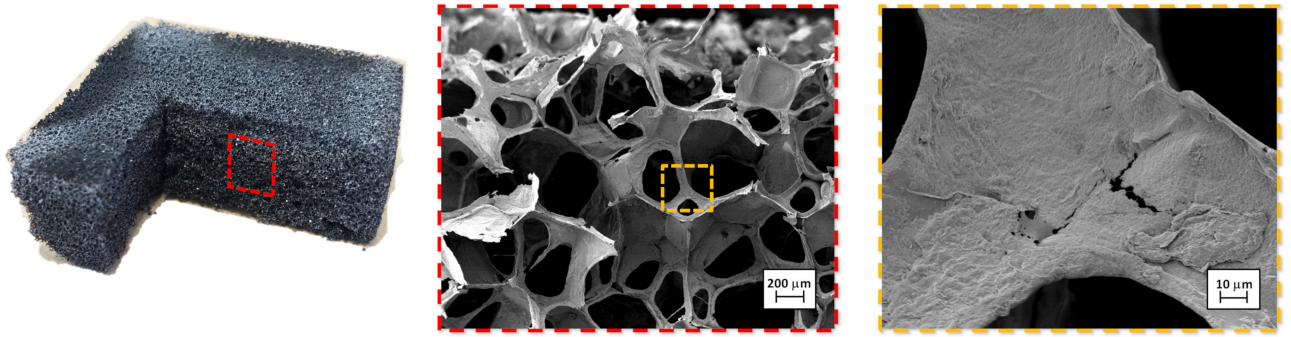

FIGURE 6 | SEM analysis (50X and 1000X) performed on the residue PU-3 L collected after cone calorimetry test.

non-compressed PU-3 L. Despite a slight detrimental effect, proportional to the number of deformation cycles observed, pkHRR values still maintain a reduction ≥40% while average smoke parameters remain within the experimental error of the PU-3 L. It seems that the cracks produced during deformation can affect the efficiency of the coating in reducing volatile release while the smoke diluting action exerted by BOH nanoparticles is mostly unaffected.

The residues collected after cone calorimetry tests have been observed by SEM (**Figure 6**). Low magnification micrographs suggest that the original 3D structure of the PU foam is left almost undamaged (compare **Figure 6** with **Supplementary Figure 2**). By increasing the magnification it is possible to reveal the real structure of the residue that mostly comprises a hollow protective exoskeleton resulting from the deposited coating. The morphology has clearly changed during combustion due to the different processes occurring within the coating (i.e., PAA degradation, BOH water release and APP decomposition) resulting in the formation of a compact barrier. The presence of cracks on the surface can be related to the release of volatiles produced by the PU that is almost completely consumed during combustion as demonstrated by the negligible change in THR values. The achieved results have been compared with other FR systems deposited on open-cell flexible PU foams by the LbL deposition of inorganic nanoparticles, natural polysaccharides or carbon nanotubes, as presented in **Figure 7**, where the best reduction in heat release rate peak achievable with each coating composition is plotted as function of the number of deposited layers (Laufer et al., 2012; Carosio et al., 2014b, 2015b, 2018b; Wang et al., 2014; Haile et al., 2016; Holder et al., 2016; Mu et al., 2017; Smith et al., 2017; Lazar et al., 2018). Red or green symbols refer to flammability and account for the ability to self-extinguish the flame and prevent its spread to the entire surface of the sample.

It can be easily appreciated that most LbL coatings can achieve substantial reductions in pkHRR (in the 40–70% range) regardless of the deposited layer number. However, in order to grant self-extinguishing behavior during flammability tests, a minimum number of 10 deposited layers is needed. This considerably reduces the efficiency of the deposited

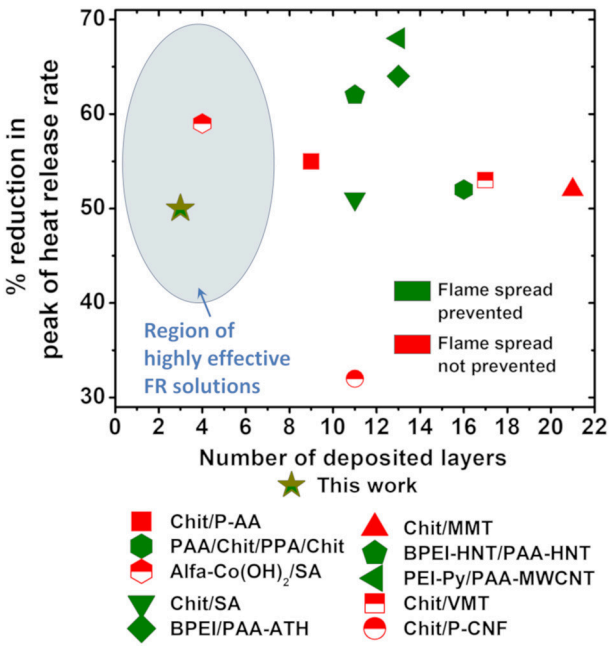

FIGURE 7 | Comparison of the flame-retardant performance in terms of peak of heat release reduction during cone calorimetry tests (35 kW/m^2). In the legend, Chit, chitosan; P-AA, phosphonated allylamine; PAA, poly(acrylic acid); PPA, poly(phosphoric acid); SA, sodium alginate; BPEI, branched polyethyleneimine; ATH, aluminum trihydroxide; MMT, montmorillonite; HNT, halloysite nanotubes; PEI-Py, pyrene functionalized polyethyleneimine; MWCNT, multi wall carbon nanotubes; VMT, vermiculite; P-CNF, phosphorylated cellulose nanofibrils.

LbL coatings and their potential applicability. On the other hand, in this paper we demonstrate that the proper design of the layer composition and the coating structure allows to achieve substantial reductions in pkHRR values (50–40%) while also obtaining self-extinguishing behavior. In addition, these characteristics are maintained after 100 deformation cycles thus confirming the potentialities of the developed solutions.

CONCLUSIONS

In this manuscript, we reported the preparation of efficient and durable layer-by-layer coatings based on the deposition of only three layers of nanoparticles containing polyelectrolytes. The deposition procedure produces a protective exoskeleton that completely covers the complex 3D geometry of the foam. The layer constituents and position have been selected on the basis of the desired flame retardant mechanism. The first layer that comprises PAA and MMT nanoplatelets produces a first barrier to volatile release. BOH nanoparticles contained in the second layer can release water with gas phase diluting and cooling effects while leaving a thermally insulating layer made of Al oxide. This latter effect is further enhanced by the third layer where APP and MMT can react together in order to produce an inorganic intumescent layer. The joint action of these three layers can stop flame spread during horizontal flammability tests leaving most of the foam undamaged (final residue up to 98% of the initial mass). Combustion rates are considerably lowered as demonstrated by a 50% reduction in pkHRR during cone calorimetry tests. Smoke production is also efficiently addressed with coated foams showing reduced smoke optical density and total smoke released. This latter aspect can prove fundamental during the evacuation of buildings in case of fire. The durability of the achieved FR performances has been evaluated by means of compression cycles. To this aim, treated foams were compressed cyclically to maximum deformation for 50 and 100 times and then their FR properties have been evaluated again. Only minor differences have been observed for the compressed foams that still exhibited excellent FR properties thus confirming the great efficiency and potential durability of the proposed coating solution. In summary, thanks to an efficient coating composition and by relying on a simple water-based approach it is possible to prepare foams capable of improving the fire safety in several applications where flexible polyurethane foams are used, including upholstered furniture and seats for households, transports, public buildings, theaters/cinemas etc.).

AUTHOR CONTRIBUTIONS

FC conceived the experiments, carried out the LbL deposition and the characterization. AF contributed to the interpretation of results and the revision of the manuscript. The manuscript was mainly written by FC.

SUPPLEMENTARY MATERIAL

The Supplementary Material for this article can be found online at: https://www.frontiersin.org/articles/10.3389/fmats.2019.00020/full#supplementary-material

REFERENCES

Ahrens, M. (2008). *Home fires that began with upholstered furniture.* Quincy, MA: National Fire Protection Association Quincy.

Alongi, J., and Carosio, F. (2016). All-inorganic intumescent nanocoating containing montmorillonite nanoplatelets in ammonium polyphosphate matrix capable of preventing cotton ignition. *Polymers* 8:430. doi: 10.3390/polym8120430

Alongi, J., Carosio, F., and Kiekens, P. (2016). Recent advances in the design of water based-flame retardant coatings for polyester and polyester-cotton blends. *Polymers* 8:357. doi: 10.3390/polym8100357

Cain, A. A., Nolen, C. R., Li, Y. C., Davis, R., and Grunlan, J. C. (2013). Phosphorous-filled nanobrick wall multilayer thin film eliminates polyurethane melt dripping and reduces heat release associated with fire. *Polym. Degrad. Stab.* 98, 2645–2652. doi: 10.1016/j.polymdegradstab.2013.09.028

Carosio, F., and Alongi, J. (2016). Ultra-fast layer-by-layer approach for depositing flame retardant coatings on flexible pu foams within seconds. *ACS Appl. Mater. Interfaces* 8, 6315–6319. doi: 10.1021/acsami.6b00598

Carosio, F., Colonna, S., Fina, A., Rydzek, G., Hemmerle, J., Jierry, L., et al. (2014a). Efficient gas and water vapor barrier properties of thin poly(lactic acid) packaging films: functionalization with moisture resistant nafion and clay multilayers. *Chem. Mater.* 26, 5459–5466. doi: 10.1021/cm501359e

Carosio, F., Di Blasio, A., Cuttica, F., Alongi, J., and Malucelli, G. (2014b). Self-assembled hybrid nanoarchitectures deposited on poly(urethane) foams capable of chemically adapting to extreme heat. *RSC Adv.* 4, 16674–16680. doi: 10.1039/C4RA01343C

Carosio, F., Di Pierro, A., Alongi, J., Fina, A., and Saracco, G. (2018a). Controlling the melt dripping of polyester fabrics by tuning the ionic strength of polyhedral oligomeric silsesquioxane and sodium montmorillonite coatings assembled through Layer by Layer. *J. Colloid Interface Sci.* 510, 142–151. doi: 10.1016/j.jcis.2017.09.059

Carosio, F., Ghanadpour, M., Alongi, J., and Wågberg, L. (2018b). Layer-by-layer-assembled chitosan/phosphorylated cellulose nanofibrils as a bio-based and flame protecting nano-exoskeleton on PU foams. *Carbohydr. Polym.* 202, 479–487. doi: 10.1016/j.carbpol.2018.09.005

Carosio, F., Kochumalayil, J., Cuttica, F., Camino, G., and Berglund, L. (2015a). Oriented clay nanopaper from biobased components–mechanisms for superior fire protection properties. *ACS Appl. Mater. Interfaces* 7, 5847–5856. doi: 10.1021/am509058h

Carosio, F., Maddalena, L., Gomez, J., Saracco, G., and Fina, A. (2018c). Graphene oxide exoskeleton to produce self-extinguishing, nonignitable, and flame resistant flexible foams: a mechanically tough alternative to inorganic aerogels. *Adv. Mater. Interfaces*. 5:1801288. doi: 10.1002/admi.201801288

Carosio, F., Negrell-Guirao, C., Alongi, J., David, G., and Camino, G. (2015b). All-polymer layer by layer coating as efficient solution to polyurethane foam flame retardancy. *Eur. Polym. J.* 70, 94–103. doi: 10.1016/j.eurpolymj.2015.07.001

Carosio, F., Negrell-Guirao, C., Di Blasio, A., Alongi, J., David, G., and Camino, G. (2015c). Tunable thermal and flame response of phosphonated oligoallylamines layer by layer assemblies on cotton. *Carbohydr. Polym.* 115, 752–759. doi: 10.1016/j.carbpol.2014.06.066

Chen, P., and Zhang, L. (2006). Interaction and properties of highly exfoliated soy protein/montmorillonite nanocomposites. *Biomacromolecules* 7, 1700–1706. doi: 10.1021/bm050924k

Decher, G., and Schlenoff, J. B. (eds.). (2012). *Multilayer Thin Films: Sequential Assembly of Nanocomposite Materials, 2nd Edn.* Weinheim: Wiley-VCH.

Dong, J., Ozaki, Y., and Nakashima, K. (1997). Infrared, Raman, and near-infrared spectroscopic evidence for the coexistence of various hydrogen-bond forms in poly (acrylic acid). *Macromolecules* 30, 1111–1117. doi: 10.1021/ma960693x

Frantzich, H. (1994). *A Model for Performance-Based Design of Escape Routes.* Department of Fire Engineering, Lund Institute of Technology, Lund University.

Gann, R. G. (2004). Estimating data for incapacitation of people by fire smoke. *Fire Technol.* 40, 201–207. doi: 10.1023/B:FIRE.0000016843.38848.37

Gómez-Fernández, S., Ugarte, L., Peña-Rodriguez, C., Zubitur, M., Corcuera, M. Á., and Eceiza, A. (2016). Flexible polyurethane foam nanocomposites with modified layered double hydroxides. *Appl. Clay Sci.* 123, 109–120. doi: 10.1016/j.clay.2016.01.015

Guido, E., Alongi, J., Colleoni, C., Di Blasio, A., Carosio, F., Verelst, M., et al. (2013). Thermal stability and flame retardancy of polyester fabrics sol-gel

treated in the presence of boehmite nanoparticles. *Polym. Degrad. Stab.* 98, 1609–1616. doi: 10.1016/j.polymdegradstab.2013.06.021

Haghnazari, N., Abdollahifar, M., and Jahani, F. (2014). The effect of NaOH and KOH on the characterization of mesoporous AlOOH nanostructures in the hydrothermal route. *J. Mexican Chem. Soc.* 58, 95–98. doi: 10.29356/jmcs.v58i2.163

Haile, M., Fomete, S., Lopez, I. D., and Grunlan, J. C. (2016). Aluminum hydroxide multilayer assembly capable of extinguishing flame on polyurethane foam. *J. Mater. Sci.* 51, 375–381. doi: 10.1007/s10853-015-9258-8

Hammond, P. T. (2004). Form and function in multilayer assembly: new applications at the nanoscale. *Adv. Mater.* 16, 1271–1293. doi: 10.1002/adma.200400760

Holder, K. M., Cain, A. A., Plummer, M. G., Stevens, B. E., Odenborg, P. K., Morgan, A. B., et al. (2016). Carbon nanotube multilayer nanocoatings prevent flame spread on flexible polyurethane foam. *Macromol. Mater. Eng.* 301, 665–673. doi: 10.1002/mame.201500327

Holder, K. M., Huff, M. E., Cosio, M. N., and Grunlan, J. C. (2015). Intumescing multilayer thin film deposited on clay-based nanobrick wall to produce self-extinguishing flame retardant polyurethane. *J. Mater. Sci.* 50, 2451–2458. doi: 10.1007/s10853-014-8800-4

Holder, K. M., Smith, R. J., and Grunlan, J. C. (2017). A review of flame retardant nanocoatings prepared using layer-by-layer assembly of polyelectrolytes. *J. Mater. Sci.* 52, 12923–12959. doi: 10.1007/s10853-017-1390-1

Klemm, D., Kramer, F., Moritz, S., Lindström, T., Ankerfors, M., Gray, D., et al. (2011). Nanocelluloses: a new family of nature-based materials. *Angew. Chem. Int. Ed Engl.* 50, 5438–5466. doi: 10.1002/anie.201001273

Kramer, R. H., Zammarano, M., Linteris, G. T., Gedde, U. W., and Gilman, J. W. (2010). Heat release and structural collapse of flexible polyurethane foam. *Polym. Degrad. Stab.* 95, 1115–1122. doi: 10.1016/j.polymdegradstab.2010.02.019

Laufer, G., Kirkland, C., Cain, A. A., and Grunlan, J. C. (2012). Clay-chitosan nanobrick walls: completely renewable gas barrier and flame-retardant nanocoatings. *Acs Appl. Mater. Interfaces* 4, 1643–1649. doi: 10.1021/am2017915

Laufer, G., Kirkland, C., Morgan, A. B., and Grunlan, J. C. (2013). Exceptionally flame retardant sulfur-based multilayer nanocoating for polyurethane prepared from aqueous polyelectrolyte solutions. *ACS Macro Lett.* 2, 361–365. doi: 10.1021/mz400105e

Lazar, S., Carosio, F., Davesne, A. L., Jimenez, M., Bourbigot, S., and Grunlan, J. (2018). Extreme heat shielding of clay/chitosan nanobrick wall on flexible foam. *ACS Appl. Mater. Interfaces* 10, 31686–31696. doi: 10.1021/acsami.8b10227

Li, Y. C., Kim, Y. S., Shields, J., and Davis, R. (2013). Controlling polyurethane foam flammability and mechanical behaviour by tailoring the composition of clay-based multilayer nanocoatings. *J. Mater. Chem. A* 1, 12987–12997. doi: 10.1039/c3ta11936j

Madejová, J. (2003). FTIR techniques in clay mineral studies. *Vib. Spectrosc.* 31, 1–10. doi: 10.1016/S0924-2031(02)00065-6

Malucelli, G., Carosio, F., Alongi, J., Fina, A., Frache, A., and Camino, G. (2014). Materials engineering for surface-confined flame retardancy. *Mater. Sci. Eng. R-Rep.* 84, 1–20. doi: 10.1016/j.mser.2014.08.001

Mohanty, A. K., Misra, M., and Drzal, L. (2002). Sustainable bio-composites from renewable resources: opportunities and challenges in the green materials world. *J. Polym. Environ.* 10, 19–26. doi: 10.1023/A:1021013921916

Mu, X., Yuan, B., Pan, Y., Feng, X., Duan, L., Zong, R., et al. (2017). A single α-cobalt hydroxide/sodium alginate bilayer layer-by-layer assembly for conferring flame retardancy to flexible polyurethane foams. *Mater. Chem. Phys.* 191, 52–61. doi: 10.1016/j.matchemphys.2017.01.023

Rawlinson, K., Dodd, V., and Sherwood, H. (2017). *Grenfell Tower Final Death Toll: Police Say 71 Lives Lost as Result of Fire*. The Guardian.

Richardson, J. J., Björnmalm, M., and Caruso, F. (2015). Technology-driven layer-by-layer assembly of nanofilms. *Science* 348, aaa2491. doi: 10.1126/science.aaa2491

Rothon, R., and Hornsby, P. (2014). "Fire retardant fillers for polymers," in *Polymer Green Flame Retardants*, eds C. Papaspyrides and P. Kiliaris (Amsterdam: Elsevier), 289–321. doi: 10.1016/B978-0-444-53808-6.00009-3

Schartel, B., and Hull, T. R. (2007). Development of fire-retarded materials—Interpretation of cone calorimeter data. *Fire Mater.* 31, 327–354. doi: 10.1002/fam.949

Smith, R. J., Holder, K. M., Ruiz, S., Hahn, W., Song, Y., Lvov, Y. M., et al. (2017). Environmentally benign halloysite nanotube multilayer assembly significantly reduces polyurethane flammability. *Adv. Funct. Mater.* 28:1703289. doi: 10.1002/adfm.201703289

Socrates, G. (2006). *Infrared and Raman Characteristic Group Frequencies - Table and Charts*. Weinheim: Wiley.

Stapleton, H. M., Klosterhaus, S., Keller, A., Ferguson, P. L., Van Bergen, S., Cooper, E., et al. (2011). Identification of flame retardants in polyurethane foam collected from baby products. *Env. Sci. Technol.* 45, 5323–5331. doi: 10.1021/es2007462

Sun, W., Liu, W.-L., and Hu, Y.-H. (2008). FTIR analysis of adsorption of poly diallyl-dimethyl-ammonium chloride on kaolinite. *J. Central South Univer. Technol.* 15, 373–377. doi: 10.1007/s11771-008-0070-3

Wang, X., Pan, Y.-T., Wan, J.-T., and Wang, D.-Y. (2014). An eco-friendly way to fire retardant flexible polyurethane foam: layer-by-layer assembly of fully bio-based substances. *RSC Adv.* 4, 46164–46169. doi: 10.1039/C4RA07972H

Conflict of Interest Statement: The authors declare that the research was conducted in the absence of any commercial or financial relationships that could be construed as a potential conflict of interest.